Forest Ecology and Management 544 (2023) 121127

Contents lists available at ScienceDirect

Forest Ecology and Management

journal homepage: www.elsevier.com/locate/foreco

Experimental drier climates affect hydraulics and induce high mortality of seedlings of three northern conifer species

Morgane Urli [a,b,1,*], Catherine Périé [b], Nelson Thiffault [a,c], Marie R. Coyea [a], Steeve Pepin [d], Travis Logan [e], Alison D. Munson [a]

[a] Université Laval, Centre d'étude de la forêt, Faculté de foresterie, de géographie et de géomatique, 2405 rue de la Terrasse, Quebec, QC G1V 0A6, Canada
[b] Direction de la recherche forestière, Ministère des Ressources Naturelles et des Forêts, 2700 Einstein, Quebec, QC G1P 3W8, Canada
[c] Canadian Wood Fibre Centre, Canadian Forest Service, Natural Resources Canada, 1055, du P.E.P.S., P.O. Box 10380, Sainte-Foy Stn., Quebec, QC G1V 4C7, Canada
[d] Université Laval, Centre de recherche et d'innovation sur les végétaux, Département des sols et de génie agroalimentaire, 2480 boul. Hochelaga, Quebec, QC, Canada
[e] Ouranos, Climate Change Consortium, Montreal, QC, Canada

ARTICLE INFO

Keywords:
Climate change
Drought-induced mortality
Hydraulic failure
Hydraulic safety margin
Northern temperate forests
Resistance to cavitation
Tree drought adaptive strategies

ABSTRACT

The future climate of northern temperate forests is projected to be drier and warmer by the end of this century. As a result, more drought-induced forest dieback events are anticipated in northeastern North America, and assessing the vulnerability of dominant tree species to drought is critical for understanding the future composition of these forests. In a greenhouse experiment, we exposed two-year-old seedlings of *Picea glauca* (Moench) Voss, *Picea mariana* (Mill.) B.S.P. and *Pinus strobus* L. to three future climate treatments for southern Quebec, Canada, and evaluated their mortality, growth, and foliage water status responses to soil water availability and atmospheric drought. Using a unique approach, climate treatments emulated droughts of different frequencies, durations, and intensities. Treatments closely simulated one growing season, with changes in air temperature and relative humidity every six hours and daily adjustment in the amount of water delivered to the seedlings. The three species experienced high mortality (75%) in all water-limited treatments compared to a control treatment that provided non-limiting soil moisture (0% mortality). The biomass of the seedlings that survived was 40% lower than that of control seedlings. Our results confirmed that the hydraulic safety margins, defined as the difference between seasonal minimum water potential and xylem water potential leading to 12, 50 and 88% of hydraulic conductivity loss, were good predictors of probability of tree mortality. Therefore, hydraulic safety margins are useful functional traits that can be used to compare the vulnerability of various species to drought and then provide crucial information to practitioners and policymakers to adjust forest management to climate change. We showed that three dominant conifer species of northern temperate forests were highly vulnerable to drought in future climates. Because drought is projected to be a significant threat to forests, understanding potentially adaptive physiological responses to drought, such as hydraulic safety margins of tree seedlings, is important for predicting the response of forest regeneration and composition in warmer and drier climates.

1. Introduction

Drought decreases tree survival, growth, and the ability of trees to cope with biotic stress (Gauthier et al., 2014; Waring, 1987) and therefore influences forest structure and composition (Brodribb et al., 2020). Significant forest dieback events have been reported worldwide (Allen et al., 2015; Hartmann et al., 2022), and are expected to increase in drier and warmer climates, even in comparatively mesic biomes (Hammond et al., 2022). Numerous boreal tree species are likely to be more sensitive to drought in the ecotone between deciduous and mixed forests in southern Quebec, Canada (Saucier et al., 2009), where species populations are at the southern edge of their distribution (Périé et al., 2009; Thompson et al., 1999). More than one third of the tree species found in southern Quebec, including *Picea glauca* (Moench) Voss, *Picea*

* Corresponding author at: Université Laval, Centre d'étude de la forêt, Faculté de foresterie, de géographie et de géomatique, 2405 rue de la Terrasse, Quebec, QC G1V 0A6, Canada.
E-mail address: urli.morgane@uqam.ca (M. Urli).
[1] Present address: Centre d'étude de la forêt, Département des Sciences Biologiques, Université du Québec à Montréal (UQAM), 141 av. du Président-Kennedy, Montréal, QC H2X 1Y4, Canada.

https://doi.org/10.1016/j.foreco.2023.121127
Received 10 March 2023; Received in revised form 14 May 2023; Accepted 17 May 2023

mariana (Mill.) B.S.P. and *Pinus strobus* L. are at risk of maladaptation to future climatic habitats (Périé and de Blois, 2016).

Climate simulations for southern Quebec based on the *Representative Concentration Pathways* (RCP) 4.5 W m^{-2} and 8.5 W m^{-2} models (Moss et al., 2010) predict an increase in mean summer temperature of 1.9 °C to 7.2 °C and a change in summer precipitation of –10% to + 12% by 2071–2100 compared to the 1971–2000 (Ouranos, 2015). These climatic conditions are expected to lead to an increase in atmospheric vapor pressure deficit (VPD), which can cause higher evapotranspiration, and hence, a decrease in soil water availability for plants (Breshears et al., 2013; McDowell and Allen, 2015). Differences in drought tolerance among species could cause shifts in the composition of this ecotone. For example, in the Upper Midwestern and Great Lakes US states, drought tolerant *Pinus* and *Quercus* species are expected to gradually replace *Populus tremuloides*, *Populus grandidentata* Michx, *Betula papyrifera* Marshall and some boreal conifer species (Clark et al., 2016). In a five-year open-air field experiment of manipulation of rainfall and temperature in Minnesota (USA), the growth and survival of juveniles of abundant species in southern boreal forests, such as *Abies balsamea* (*Linnaeus*) Miller and *P. glauca* were reduced when the treatments represented climatic conditions outside their climate envelope (Reich et al., 2022). In contrast, the responses of *Acer* and *Quercus* to these treatments suggested climate change may have initially positive impacts on these species, potentially allowing replacement conifer species on these ecotones (Reich et al., 2022).

Trees experiencing water stress respond to increased VPD by closing their stomata to maintain xylem water potential above a critical threshold (Martin-StPaul et al., 2017). Stomatal closure affects photosynthesis and transpiration and therefore alters the balance between carbon gain and water loss. The longer the exposure to drought, the more depleted the carbon reserves become, and the more likely a tree will die from carbon starvation (McDowell et al., 2008). Moreover, as the atmospheric or soil water deficit becomes more intense, the xylem water potential decreases and the risk of failure of the hydraulic system through cavitation increases (Stroock et al., 2014). Therefore, species-specific combinations of hydraulic failure, carbon starvation, and enhanced vulnerability to secondary biotic attacks are the main mechanisms leading to drought-induced tree mortality (Anderegg et al., 2015; McDowell et al., 2022).

In this context, there is a need to assess mortality, growth and physiological responses of boreal and northern temperate tree species in future warmer and drier conditions. Extreme tree mortality events induced by drought were observed in the recent past in forests dominated by sugar maple (*Acer saccharum* Marsh)-red oak (*Quercus rubra* L.) forests in southern Quebec (Ministère des Ressources naturelles (2012), personal communication, Alison Munson and Carine Annecou). However, responses of tree water status of these species to drought, including their hydraulic safety margin, are poorly understood (Balducci et al., 2015; Hajek et al., 2022). Although timing of tree mortality during a drought event is difficult to predict, numerous studies provide evidence that hydraulic failure and tree mortality are closely linked (Adams et al., 2017b; Anderegg et al., 2016; Brodribb et al., 2020; Brodribb and Cochard, 2009; Brodribb et al., 2010; Choat et al., 2018; Skelton et al., 2017; Urli et al., 2013). Therefore, mortality risk of different species under drought conditions could be assessed by measuring tree hydraulic safety margins (Delzon and Cochard, 2014). This margin is the difference between the maximum level of shoot water stress experienced during a growing season (*i.e.,* the seasonal minimum water potential, ψ_{min}) and the water potential leading to 12, 50 or 88% loss of conductivity (Meinzer et al., 2009).

We studied three conifer species (*P. glauca*, *P. mariana* and *P. strobus)* of major ecological and economic importance, for which changes in distribution and dynamics could make entire ecosystems and economies vulnerable. *Picea* species are widely planted across Canada, including in southern Québec; they are valued for high-quality pulp and paper making (Burns and Honkala, 1990). *P. strobus* is being restored in several regions, since it was a dominant component of the pre-industrial southern hardwood and mixed forests, providing wood that is valued for industries such as furniture making (Laflamme et al., 2016). Together, these three species represent 79.5% of the seedlings planted in Québec in the last decade (Ministère des Forêts de la Faune et des Parcs, 2020). In a greenhouse experiment, we exposed two-year-old seedlings of *P. glauca*, *P. mariana* and *P. strobus* to four simulated growing season climate regimes that include three water-limited (WL) treatments and a well-water control. Our objectives were to assess: (*i*) seedling growth and mortality; and (*ii*) the mortality risk induced by drought as estimated by the hydraulic safety margin. We addressed the following question: will two WL treatments with a similar level of cumulative water stress, but differently distributed during the growing season (a drought of high intensity vs. frequent droughts of lower intensity), similarly affect species with different degrees of isohydry? We hypothesized (i) that *P. strobus*, with its more isohydric strategy would show better survival and growth and lower levels of hydraulic dysfunction in the WL treatment with drought of high intensity than in the treatment with frequent droughts of lower intensity; and (ii) that the *Picea* species would show the opposite behavior.

2. Materials and methods

2.1. Plant materials

During the autumn 2018, two-year-old container seedlings were allowed to cold harden outside at < 10 °C and then placed in a cold chamber at –2 °C to accumulate the required number of chilling degree days to break bud dormancy. Seedlings came from seeds from a single seed orchard per species (*P. glauca*: 46° 02′ 05″ N, 73° 11′ 38″ W, *P. mariana*: 46° 41′ 02″ N, 72° 40′ 48″ W, *P. strobus*: 45° 41′ 32″ N, 73° 19′ 48″ W) and are adapted to the sugar maple-yellow birch bioclimatic domain.

2.2. Experimental design

In December 2018, seedlings were transplanted into 3.53 L cylindrical plastic containers (high density polyethylene, Classic 300, Nursery Supplies) filled with a mixture of peat moss, fine perlite and vermiculite (v:v:v, 3:1:1). Fifteen grams of slow-release fertilizer (ACER® nt 13-10-15) was applied and the soil surface was covered with silica to minimize evaporation. The 224 seedlings per species were distributed across four greenhouse compartments (*i.e.*, treatments) at Université Laval in Quebec City. Fifty-six seedlings per species were arranged in a randomized block design (four blocks) within each treatment. Each variable (except survival) was measured several times during the growing season on one seedling per block (4 blocks for all variables except 3 blocks for hydraulic conductivity and biomass), species, and treatment. The experimental unit was the seedling. After a minimum of two weeks of acclimation, four climatic conditions (or treatments, one per compartment) were applied starting January 1, 2019, for a period of four months, to simulate the climate of future growing seasons from June to September. These four treatments were created by controlling air temperature and relative humidity, and by applying a controlled volume of water to the seedlings to simulate projected precipitation regimes for the three WL treatments and a well-watered regime for the control. The three WL treatments presented a gradient of cumulative water deficit at the end of the growing season with different drought intensities and frequencies during the season. Supplementary lighting by 400 W, high pressure sodium lamps (PL Light Systems, Beamsville, ON, Canada) were used to provide a natural growing season photoperiod. Photosynthetic photon flux density (PPFD) measured at mid-seedling level was ~ 285 μmol m^{-2} s^{-1}, which is typical of the understory PPFD conditions.

2.3. Climate treatments

We exposed seedlings to three WL treatments (WL1, WL2, WL3) created to simulate future growing season (May-September) climates for the sugar-maple-yellow birch domain. A fourth control treatment (Control) provided non-limiting soil moisture conditions. The experimental design was unique in that seasonal variability in atmospheric evaporative demand (as measured by VPD) and soil moisture availability was created by changing air temperature and relative humidity every 6 h, and by applying a specific volume of water to each pot every day (Fig. 1).

The WL1 simulated the climate conditions that occurred in 2012, between May and September, in the region where trees experienced a severe drought (Agriculture et Agroalimentaire Canada, 2012) after which significant tree dieback was noted by several observers (Ministère des Ressources naturelles (2012), personal communication, Alison Munson and Carine Annecou). The air temperature, relative humidity, and precipitation applied in this greenhouse compartment were based on the weather station data near Ottawa, Ontario, Canada (n°6106001, 45° 19′ N, 75° 40′ W; Environment and Climate Change Canada, 2018).

The WL2 and WL3 treatments were developed based on a range of climate simulation projections of maximum growing season water deficit produced from four Canadian Regional Climate Model (CRCM 5) simulations (Table S1, Martynov et al., 2013; Šeparović et al., 2013). Simulations were performed using the RCP 8.5 W m^{-2} future greenhouse gas projected evolution (Meinshausen et al., 2011). A nearest-neighbor selection of the model grid cell closest to the centroid of the observed weather station data was performed to select data for the two treatments, which were (*i*) WL2 treatment simulating the potential future conditions of this geographical region based on the observed seasonal variability of 2012 and an anomaly of temperature and precipitation derived from the CRCM 5 simulations and; (*ii*) WL3 treatment simulating the future conditions of a single year selected from the 2071–2100 horizon, with the seasonal variability given directly from the CRCM 5 simulations.

For the WL2 and WL3 treatments, water balance (mm), defined as the difference between precipitation and potential evapotranspiration, was used to select a single representative simulated future year for the determination of treatments. This selection was made by determining the simulated year between 2071 and 2100 whose maximum cumulated water deficit fell closest to the 10th percentile of all future years (n = 120: 30 years – 2071–2100 – × 4 CRCM 5 simulations). To calculate the maximum cumulated water deficit, we first estimated daily potential evapotranspiration following the equation of Baier and Robertson (1965) modified by Rochette and Dubé (1989). Subsequently, daily water balance (total precipitation minus evapotranspiration) was determined for each simulated year starting from June, 1. The cumulative water deficit (mm) and its occurrence date were then calculated based on the sum of daily water balance during the growing season.

Simulated daily temperature, precipitation, and relative humidity values of the selected year were used directly for the WL3 treatment. For the WL2 treatment, temperature and precipitation anomalies for the selected future year were determined based on the mean values from 1986 to 2005 as follows:

$$anomT_{y,m} = \left(T_{y,m} - T_{m1986-2005}\right) - anomT_{obs2012,m}$$

$$anomP_{y,m} = \left(\left(P_{y,m}/P_{m1986-2005} - 1\right) \times 100\right) - anomP_{obs2012,m}$$

where $anomT_{y,m}$ is the temperature anomaly for year y and month m (°C), $anomP_{y,m}$ is the precipitation anomaly for year y and month m (%), $T_{y,m}$ is the value of the temperature for the year y and the month m, $T_{m1986-2005}$ is the mean value of simulated temperature for the period 1986–2005 for month m, $anomT_{obs2012}$ is the observed temperature anomaly for year 2012 and month m calculated using data from the weather station, $P_{y,m}$ is the value of precipitation for year y and month m, $P_{m1986-2005}$ is the mean value of simulated total precipitation for the period 1986–2005 for month m and $anomP_{obs2012}$ is the observed precipitation anomaly for year 2012 and month m calculated using data from the weather station. The observed temperature and precipitation anomalies of year 2012 were subtracted since 2012 was drier and hotter than the mean of observed conditions. Monthly temperature and precipitation anomalies were then linearly interpolated to daily values and applied to observed 2012 station data to create future conditions. WL2 relative humidity values remained the same as those of the WL1 treatment, because the anomalies of relative humidity obtained with the same method as air temperature or precipitation, were less than the level of control of the relative humidity in the greenhouse.

In the Control treatment, air temperature and relative humidity were the same as in the WL1 treatment, but soil moisture was maintained at container capacity. During the acclimation period, all four treatments maintained the temperature, light and relative humidity conditions found in the same southern Quebec geographical region as in May 2012, but with soil water at container capacity.

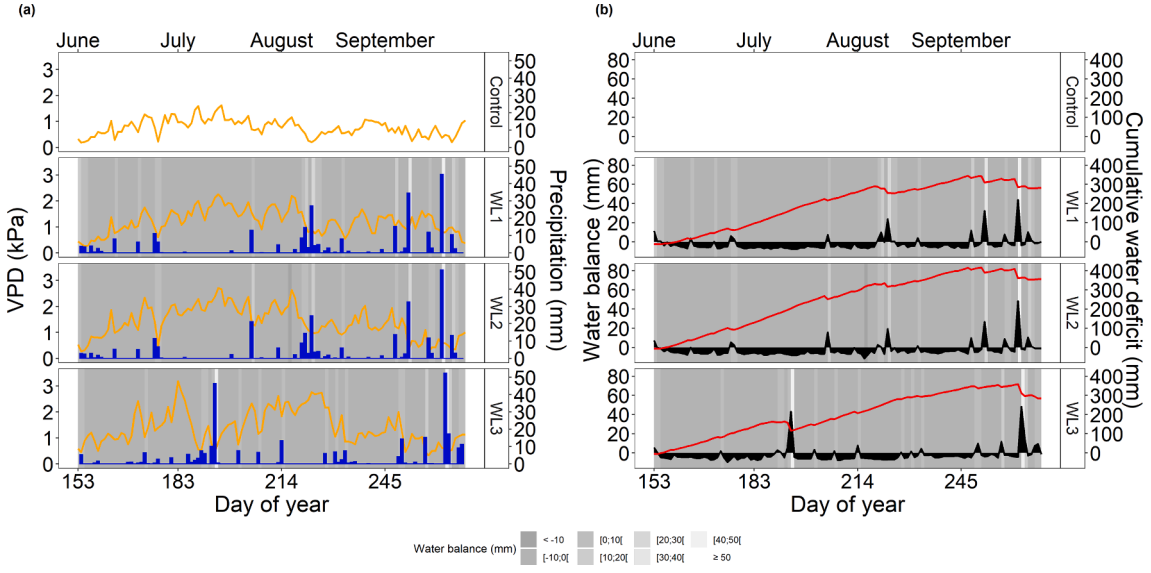

Fig. 1. Observed daily (a) vapor pressure deficit (VPD, orange line), precipitation (blue bars), (b) water balance (black shading) and cumulative water deficit (red line) in the four treatments.

For each WL treatment, the daily water balance, value and date of the maximum cumulated water deficit were calculated (Table 1, Fig. 1). We also determined the probability of occurrence of a climate with higher maximum water deficit for the periods 2041–2070 and 2071–2100 among the simulated years with the RCP 4.5 W m^{-2} and the RCP 8.5 W m^{-2} (Table 1).

2.4. Mortality, ecophysiological measurements and growth

Mortality was visually assessed three times during the experiment: at the beginning of the experiment after transplantation (early June), in the middle of the growing season (mid-August), and at the end of the season (late September). Seedlings were considered as dead when their needles, stems and buds were dry visually and to the touch as well as unresponsive to pressure chamber measurements.

The ecophysiological measurements began when needles of all plants in each treatment were fully expanded. They ended when foliage water potential (ψ) could no longer be measured due to needle desiccation. Volumetric soil water content (θ_v, $m^3\ m^{-3}$), predawn and midday ψ (respectively, ψ_{pd} and ψ_{md}, MPa), stem-specific hydraulic conductivity (K_s, kg $m^{-1}\ s^{-1}\ MPa^{-1}$) and oven-dry shoot and root biomass (B_{shoot} and B_{root}, g) were measured several times during the growing season (12 measurements in the WL treatments and six measurements in the Control for θ_v, ψ and K_s, and six measurements in the WL and Control treatments for, B_{shoot} and B_{root}). For each treatment and measurement, the day of measurement corresponded to the same day of the year (DOY) of a simulated future climate, except for the last two measurements, which, for technical reasons, were performed on different DOYs: DOY = 256 for WL3 and DOY = 257 for WL1 for the second to last measurement and DOY = 263 for WL3 and DOY = 267 for Control and WL1. Water potential was measured with a Scholander pressure chamber (Model 1505-EXP, PMS Instrument Company, Albany, OR, USA) on at least four seedlings of each species, for each treatment and measurement, on foliage from the previous growing season, *i.e.*, on twigs (stem + needles) of seedlings for *Picea* species (because of the small size of their needles) and on needles, placed inside foil bags at least 30 min before ψ_{md} were performed, for *P. strobus* (to obtain ψ of twigs). Seedlings were illuminated with a LED light (SK602GH, Spectrum King Grow Lights, Los Angeles, CA, USA) for at least 45 min before measuring ψ_{md} (PPFD ~ 580 μmol $m^{-2}\ s^{-1}$ at mid-seedling height) to ensure that ψ_{md} was measured under non-light limiting conditions. Volumetric soil water content (θv) was calculated by multiplying the gravimetric soil water content by the ratio of the bulk density of the soil to the water density. K_s, B_{shoot} and B_{root} were measured on at least three of the seedlings on which ψ was measured. Roots and shoots were dried at 60 °C in an oven for at least 72 h and then weighed (Cornelissen et al., 2003). Oven-dry total biomass and root:shoot ratio were calculated as the sum of B_{shoot} and B_{root} and the ratio between B_{root} and B_{shoot}, respectively.

We used a custom-built flowmeter following the protocol of Sack et al. (2011) to measure the stem-specific hydraulic conductivity of a debarked segment, cleaned with 70% alcohol solution and cut 4–6 cm from the basis of the main stem axis. Flow rate through the segment (Q, kg s^{-1}) was determined by the drop in pressure across a tube of known hydraulic resistance (cf. Melcher et al. (2012) for more details). Degassed, filtered (0.45 μm) distilled and purified (Barnstead E-Pure; Thermo Scientific, Waltham, MA, USA) water containing KCl (10 mM) and $CaCl_2$ (1 mM) was used as a perfusing solution during measurements. Flow for each sample was the mean of consecutive 5 s interval measurements made during the last 5 min when steady-state rate was achieved, standardized to 25 °C.

Seedlings of the Control treatment were never water stressed. Therefore we used the mean species stem-specific hydraulic conductivity of those seedlings per month (to account for seedling growth) as maximum hydraulic conductivity to assess the native embolism (*i.e.*, the percent loss of hydraulic conductivity, *PLC*, %) in the WL treatments. We calculated the *PLC* of a seedling i of WL treatment j, species k measured during the month l (June to September) as follows:

$$PLC_{i,j,k,l} = \left(1 - \frac{K_{s_{i,j,k,l}}}{\overline{K_{s_{Control,k,l}}}}\right) \times 100$$

When $K_{s_{i,j,k,l}} > \overline{K_{s_{Control,k,l}}}$, we used the maximum value of $K_{s_{Control,k,l}}$ as maximum hydraulic conductivity.

2.5. Vulnerability curves and hydraulic safety margins

We built the hydraulic vulnerability curves of each species using pot and bench dehydration methods with seedlings of the same age, seed provenance and potting substrate as in the main experiment. Since there was no significant difference in P_{12}, P_{50} and P_{88} values between both methods (Urli et al., under review), we fitted a unique vulnerability curve per species, combining data from both methods on the relationship between K_s and the stem xylem water potential with a Weibull function. The maximum K_s was defined as the measured K_s between –1 and 0 MPa because the plants were always grown in well-watered conditions before the beginning of the experiments. Vulnerability curve parameters – P_{12}, P_{50} and P_{88} – and their bootstrapped 95% confidence intervals were estimated using the *fitplc* package (Duursma and Choat, 2017) in R version 4.0.2 (R Core Team, 2020). Absence of overlap between confidence intervals between species was taken as

Table 1
Mean values (±SE) of daily minimum temperature (Tmin), daily maximum temperature (Tmax) and vapor pressure deficit (VPD), total precipitation (P) during the growing season, value (mm) and date of the maximum (max.) cumulated water deficit using the equation of Baier and Robertson (1965) modified by Rochette and Dubé (1989) (cf. Materials and Methods) and the probability of occurrence of a climate with higher maximum water deficit for two periods 2041–2070 and 2071–2100 based on RCP 4.5 W m^{-2} and RCP 8.5 W m^{-2} simulations (Meinshausen et al., 2011) for each treatment (WL1, WL2 and WL3 simulated the climate conditions that occurred during the growing season of 2012 for the sugar-maple-yellow birch domain, the potential future conditions of this geographical region based on the observed seasonal variability of 2012 and, the future conditions of a single year selected from the 2071–2100 horizon respectively. The Control treatment is based on the WL1 treatment but with soil moisture maintained at container capacity, that is, non-limiting moisture).

Treatment	*Tmin* (°C)	*Tmax* (°C)	VPD (kPa)	P (mm)	Max. cumulated water deficit (mm)	Date of max. cumulated water deficit	Probability of occurrence of a climate with higher maximum water deficit			
							2041–2070 RCP 4.5 W m^{-2}	2071–2100 RCP 4.5 W m^{-2}	2041–2070 RCP 8.5 W m^{-2}	2071–2100 RCP 8.5 W m^{-2}
Control	12.75 (±0.18)	23.96 (±0.22)	0.68 (±0.02)							
WL1	13.19 (±0.19)	24.18 (±0.24)	1.06 (±0.03)	374	345	Sept. 3	0.43	0.41	0.48	0.53
WL2	15.88 (±0.22)	27.01 (±0.29)	1.14 (±0.04)	377	417	Sept. 9	0.21	0.17	0.23	0.32
WL3	16.87 (±0.23)	27.00 (±0.26)	1.19 (±0.04)	354	359	Sept. 18	0.39	0.35	0.42	0.49

evidence that significant difference in P_{12}, P_{50} or P_{88} were exhibited.

For each species and water-limited treatment, hydraulic safety margins (MPa) were determined as the difference between seasonal minimum water potentials (ψ_{min}, MPa) during the growing season and P_{12}, P_{50} or P_{88}, respectively (Meinzer et al., 2009). Seasonal minimum water potential values were determined as ψ_{md} values lower than the 10th quantile of the distribution of ψ_{md} for each species and WL treatment. When only ψ_{pd} could be measured for a seedling, we used ψ_{pd} as a proxy for ψ_{md} for the determination of ψ_{min}. Predicted PLC (PLC_p) of each species and WL treatment was defined as the percent loss of conductivity induced by ψ_{min} and was calculated using the vulnerability curve of each species.

2.6. Statistical analyses

Analyses of variance (ANOVA) were used to examine the responses of survival rate, total biomass, root:shoot ratio, θ_v, ψ_{pd}, ψ_{md} and the native embolism (*PLC*) to treatment, species and time, their three two- and the three-way interactions. Time was considered as a categorical variable (month for survival rate (n = 3) and for *PLC* (n = 4), and DOY for total biomass, root:shoot ratio, θ_v, ψ_{pd} and ψ_{md}). Analyses were conducted with (*i*) generalized linear mixed-effects models (GLMM) with 'block' nested in 'treatment' as random effects to analyze the responses of survival rate with a binomial distribution of the residuals and (*ii*) linear mixed-effects models (LMMs) to analyze the responses of total biomass, root:shoot ratio, θ_v, ψ_{pd}, ψ_{md} and *PLC* with 'block' nested in 'treatment' as random effects. A compound symmetry matrix was used as the variance–covariance matrix of the error terms for all models. A GLMM with 'block' nested in 'treatment' as random effects with a binomial distribution of the residuals was used for the analysis of survival rate, since a GLMM with repeated measures with 'block' nested in 'treatment' and 'seedling id' as random effects and a binomial distribution of the residuals did not converge.

We performed ANOVAs to analyze the responses of ψ_{min}, PLC_p and hydraulic safety margins to WL treatments, species and the two-way interaction. These analyses were conducted with linear models.

For the LMMs, degrees of freedom associated to the denominators for the tests of fixed-effects were calculated with the Satterthwaite method, as the factors associated to the random effects had few levels and the distribution of their estimators was better approximated by a χ^2 distribution than a normal distribution (Littell et al., 2006).

Post-hoc multiple mean comparisons were tested with Bonferroni tests, except when the three-way interaction was significant.

In all analyses, we conducted standard procedures for model diagnostics. When normality and homoscedasticity of the data were not met, we transformed the data using the natural logarithm. All analyses were conducted using R version 4.0.2 (R Core Team, 2020), with the *lme4* package for GLM and GLMM (Bates et al., 2015), the *lmerTest* package (Kuznetsova et al., 2017) for LMMs, and *emmeans* package (Lenth, 2021) for post-hoc tests.

3. Results

3.1. Survival rate and oven-dry total biomass during the growing season

Survival rate significantly differed with treatment, species, time and the two-way interactions treatment × time and species × time (Table 2). Survival rate decreased with time for all species in all treatments except the Control (Fig. 2a). The survival of *P. mariana* decreased more rapidly with time than *P. glauca* and *P. strobus* (Fig. 2b). At the end of the experiment, survival rate of *P. mariana* was lower than *P. strobus* but similar to *P. glauca* (Fig. 2b). Survival rate in the WL2 treatment was lower than that in the WL3 treatment but similar to that in the WL1 treatment. In all cases, for these three WL treatments, survival was at most 25%.

Total biomass varied significantly with treatment, species, time, and the two-way interaction treatment × time (Table 2). *P. strobus* presented the lowest total biomass of the three species (Fig. 3a) and its root:shoot

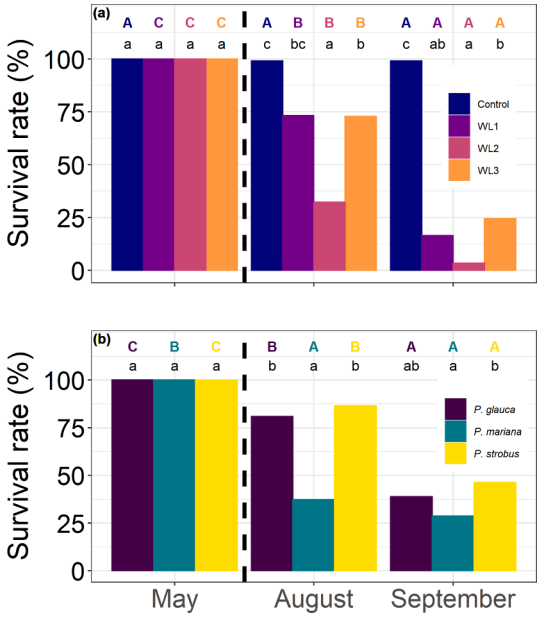

Fig. 2. Change in seedling survival rate over time for (a) treatments and (b) species. Survival rate sharing the same lower-case letter indicates no significant difference within a monthly period ($\alpha < 0.05$). Survival rate sharing different colored upper-case letters denotes significant differences between months ($\alpha < 0.05$). The vertical dashed line is provided to indicate the x-axis is discontinuous.

Table 2
ANOVA results for survival rate (%), oven-dry total biomass (g) and native embolism (*PLC*, %) among treatments (WL treatments for *PLC*), species and time*. Values in bold indicate a significant effect at $\alpha < 0.05$.

	Survival rate			Oven-dry total biomass			*PLC*		
	Df	χ^2	*P*	Df[a]	*F*	*P*	Df[a]	*F*	*P*
Treatment	3	75.86	**<0.001**	3, 12.55	18.946	**<0.001**	2, 183	4.788	**0.009**
Species	2	56.074	**<0.001**	2, 112.66	51.461	**<0.001**	2, 183	0.852	0.428
Time	2	214.011	**<0.001**	5, 112.24	53.153	**<0.001**	3, 183	15.522	**<0.001**
Treatment × Species	6	4.392	0.632	6, 112.12	1.293	0.266	4, 183	0.094	0.584
Treatment × Time	6	46.775	**<0.001**	12, 112.00	5.101	**<0.001**	5, 183	0.508	0.770
Species × Time	4	21.642	**<0.001**	10, 111.74	1.528	0.139	6, 183	0.860	0.525
Treatment × Species × Time	12	5.966	0.918	21, 112.05	1.170	0.290	9, 183	1.254	0.265

*Time was considered as categorical variable (month for survival rate (n = 3) and for *PLC* (n = 4) and day of year (DOY) for oven-dry total biomass). The last measurement run was performed on different DOYs for different treatments: DOY = 263 for WL3 treatment and DOY = 267 for Control and WL1 treatments. Because these DOY did not differ by more than 3 days, total biomass of the last measurement run was analyzed as if it was measured the same DOY between treatments.

[a] Degrees of freedom presented as numerator, denominator. Denominator degrees of freedom were calculated with the Satterthwaite method (Littell et al., 2006).

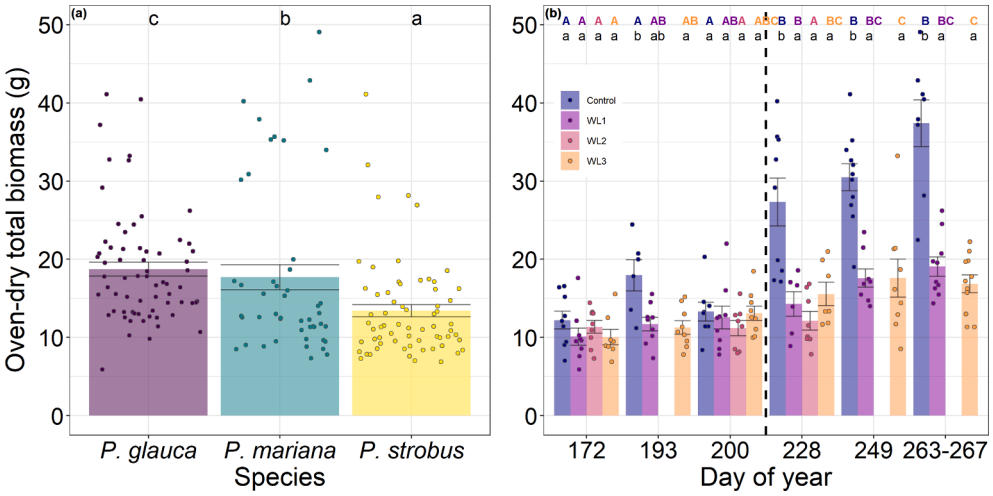

Fig. 3. (a) Difference in mean oven-dry total biomass among species. Means sharing the same lower-case letter indicate no significant difference ($\alpha < 0.05$). (b) Change in mean oven-dry total biomass of seedlings over time for treatment. Means sharing the same lower-case letter indicate no significant difference within a day of year ($\alpha < 0.05$). Means sharing colored upper-case letters denote significant differences between days of year within a treatment. Bar plots show mean ± SE and jitter represents the distribution of the underlying data ($n \leq 67$ seedlings for (a) and $n \leq 11$ seedlings for (b)). The vertical dashed line is provided to indicate the x-axis is discontinuous.

ratio decreased during the growing season for the WL treatments (Fig. S1). However, this ratio was higher than those of the *Picea* species in most WL treatment × time combinations, except at the end of the experiment (Fig. S1, Table S2). Total biomass of all species increased more rapidly in the Control than in the WL treatments, whereas the total biomass did not differ among the WL treatments during the growing season (Fig. 3b). At the end of the growing season, the total biomass of seedlings that survived in the WL treatments was 40% lower than that observed in the Control.

3.2. Soil water content and xylem water potentials during the growing season

The θ_v, ψ_{pd} and ψ_{md} fluctuated during the growing season and differed among species (significant species × time interaction, Fig. 4, Table S3). Moreover, this interaction between species and time differed among treatments (significant three-way interaction species × treatment × time, Fig. 4, Table S3). θ_v, ψ_{pd} and ψ_{md} fluctuated little during the growing season in the Control compared to the WL treatments (significant effect of treatment × time, Fig. 4, Table S3). Indeed, ψ of species in the Control were greater than –1 MPa and –1.25 MPa for ψ_{pd} and ψ_{md}, respectively, as θ_v was maintained close to container capacity during the

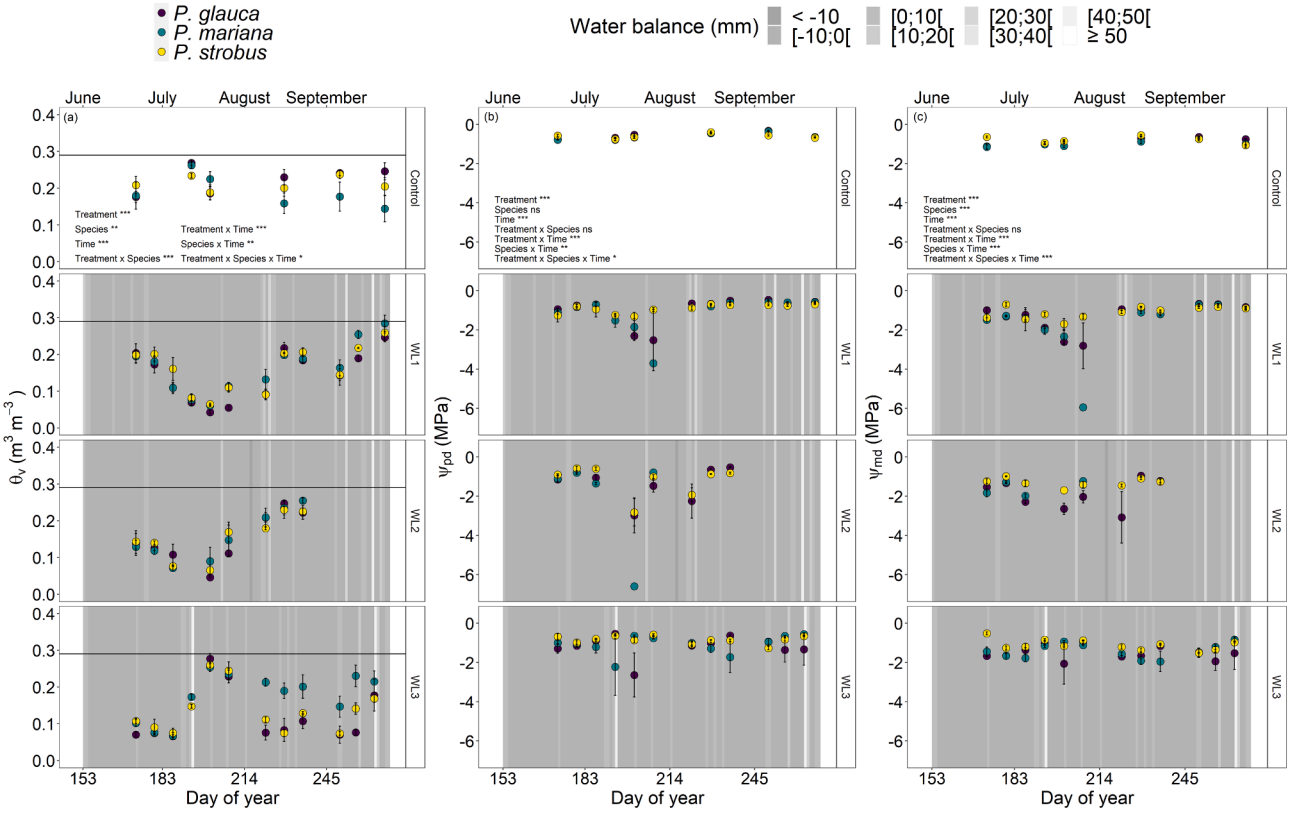

Fig. 4. Change in mean (a) soil water content (θ_v), (b) predawn water potential (Ψ_{pd}) and (c) midday water potential (Ψ_{md}) over time for species and treatment. Data are presented as mean ± SE ($n \leq 8$ seedlings). Horizontal black lines indicate the value of soil water content at maximum container capacity. Results of ANOVA are indicated for each variable (ns: non significant; *: $P < 0.05$; **: $P < 0.01$; ***: $P < 0.001$).

growing season in this treatment (Fig. 4). In the WL1 and WL2 treatments, θ_v, ψ_{pd} and ψ_{md} of the three species decreased between mid-June and mid-July, corresponding to a period of drought (Fig. 1); this decrease of ψ, especially of ψ_{md}, was higher for *Picea* species than for *P. strobus* in both treatments. During the most extreme part of the drought on July 19, average ψ_{md} was –2.61 ± 0.14, –2.34 ± 0.32 and –1.69 ± 0.29 MPa for *P. glauca*, *P. mariana* and *P. strobus,* respectively, in the WL1 treatment and –2.64 ± 0.29 and –1.69 MPa for *P. glauca* and *P. strobus,* respectively, in WL2 treatment (Fig. 4). ψ_{md} measurements for *P. mariana* were not possible at that time, but one seedling showed ψ_{pd} = –6.6 MPa. Recovery phases were detectable for all species in these treatments, with increases in θ_v and ψ from the end of the drought period until the end of the experiment. However, ψ levels for *Picea* species remained low during the recovery period, particularly after the simulated rainfall on July 23 in the WL1 treatment (see Fig. 4).

No clear period of drought was observed in the WL3 treatment, as the distribution of precipitation across the growing season was more regular than in the other WL treatments (Fig. 1). Nevertheless, the three species exhibited lower values of θ_v and of both ψ_{pd} and ψ_{md} in this treatment than in Control treatment (Fig. 4).

The variability of ψ increased with water stress experienced by seedlings in all WL treatments, for all species, but especially for *Picea* species (Fig. 4, Fig. S2).

3.3. Vulnerability curves

P. glauca (P_{50} = –2.29 [–2.41; –2.21] MPa, P_{88} = –2.61 [–3.09; –2.46] MPa) was significantly more vulnerable to cavitation than *P. mariana* (P_{50} = – 3.01 [–3.37; –2.77] MPa, P_{88} = –3.74 [–4.30; –3.15] MPa) and *P. strobus* (P_{50} = –3.21 [–4.21; –2.60] MPa, P_{88} = –4.93 [NA; –3.13] MPa) (Fig. 5). Moreover, K_s of *P. mariana* and *P. strobus* decreased more slowly with decreasing water potential than *P. glauca*. Therefore, P_{12} of *P. glauca* (P_{12} = –1.86 [–2.03; –1.50] MPa) was not significantly different from that of *P. mariana* (P_{12} = –2.17 [–2.51; –1.91] MPa) and *P. strobus* (P_{12} = –1.68 [–2.82; –1.10] MPa).

3.4. Native embolism, predicted PLC and hydraulic safety margins

Only treatment and time had a significant effect on native embolism (*PLC*) (Table 2). *PLC* values in all WL treatments exceeded 12%, with seedlings in the WL2 treatment having higher *PLC* (~40%) than in the other WL treatments (~27%; Table 2, Fig. 6a). *PLC* and its variability among seedlings increased throughout the growing season for all species and WL treatments with *PLC* < 50% for almost every seedling in June; only eight seedlings exhibited a *PLC* < 12% in August and September (Fig. 6b, Table 2).

The interaction treatment × species was not significant on ψ_{min} and PLC_p ($F_{4,29}$ = 0.885, P = 0.485 for ψ_{min} and $F_{4,29}$ = 0.493, P = 0.741 for PLC_p). *P. strobus* had higher ψ_{min} (less negative) than *Picea* species ($F_{2,29}$ = 8.455, P = 0.001, Fig. 7a) and exhibited PLC_p < 50% contrary to the *Picea* species. Indeed, no seedling of *P. strobus* exhibited a $\psi_{md} < P_{50}$ whatever the treatment (Fig. S2). *P. glauca* showed significantly higher PLC_p than *P. mariana* and *P. strobus* ($F_{2,29}$ = 15.069, P < 0.001, Fig. 7c). The seedlings in the WL2 treatment showed significantly lower ψ_{min} and higher PLC_p (not significant) than those in the WL3 treatment ($F_{2,29}$ = 4.567, P = 0.019 for ψ_{min} and $F_{2,29}$ = 1.934, P = 0.163 for PLC_p, Fig. 7b, d). Despite the variability of PLC_p among seedlings, all seedlings from all species and WL treatments exhibited $PLC_p \geq 12\%$. Whatever the level of water stress used to estimate the hydraulic safety margins (P_{12}, P_{50} or P_{88}), the effect of the treatment × species interaction did not influence its value ($F_{4,29}$ = 0.280, P = 0.889, $F_{4,29}$ = 0.280, P = 0.889 and $F_{4,29}$ = 0.280, P = 0.889 for $\psi_{min} - P_{12}$, $\psi_{min} - P_{50}$ and $\psi_{min} - P_{88}$, respectively). The effects of the WL treatments were marginally significant on hydraulic safety margins defined with P_{12} and P_{50} ($F_{2,29}$ = 3.587, P = 0.041 and $F_{2,29}$ = 3.214, P = 0.054 for $\psi_{min} - P_{12}$ and $\psi_{min} - P_{50}$, respectively) with the lowest margins measured in the WL2 treatment (Fig. 7f, h) and not significant for $\psi_{min} - P_{88}$ ($F_{2,29}$ = 2.724, P = 0.082). $\psi_{min} - P_{12}$, $\psi_{min} - P_{50}$ and $\psi_{min} - P_{88}$ were significantly different among species ($F_{2,29}$ = 4.052, P = 0.028, $F_{2,29}$ = 12.445, P < 0.001 and $F_{2,29}$ = 30.065, P < 0.001). All species exhibited a negative $\psi_{min} - P_{12}$ whatever the WL treatment (Fig. 7e). $\psi_{min} - P_{50}$ and $\psi_{min} - P_{88}$ were negative (or equal to 0) for *Picea* species but positive for *P. strobus* (Fig. 7g, i). However, the calculation of the hydraulic safety margin did not consider the confidence intervals of P_{12}, P_{50} and P_{88}. Therefore, $\psi_{min} - P_{50}$ and $\psi_{min} - P_{88}$ of *P. strobus* in the WL1 treatment could be closer to 0 (cf. little diamond symbols in Fig. 7).

4. Discussion

4.1. Drought-induced mortality of seedlings in warmer and drier climatic conditions

The mortality rate above 75% whatever the species and the treatments suggests that at the seedling stage, these species are highly vulnerable to hotter drought in future climates of southern Quebec. Hotter drought is likely to be a main factor limiting regeneration success and survival of these three species in southern Quebec by the end of this century, and therefore, leading to the predicted loss of climatically favorable habitats in southern Quebec (Périé and de Blois, 2016). Indeed, the high mortality for *P. glauca* and *P. mariana* in response to the

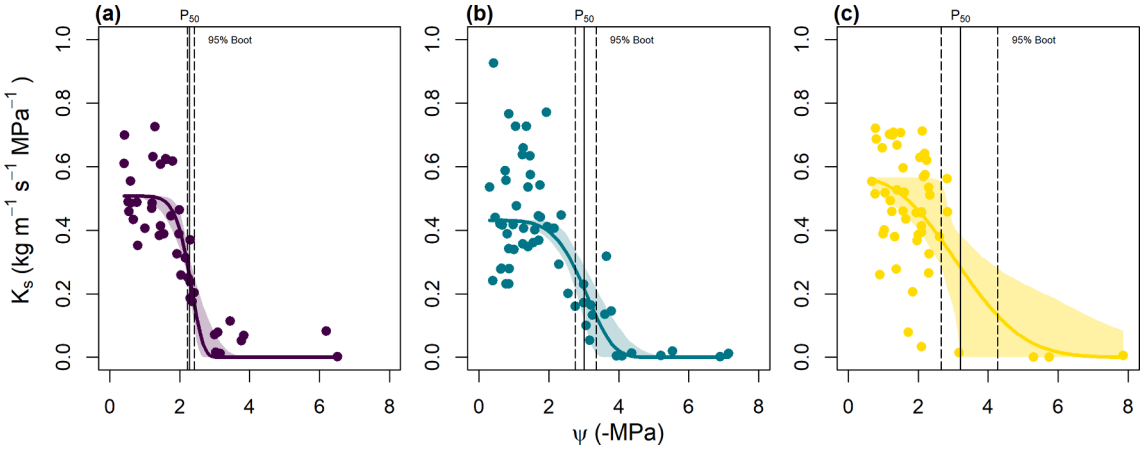

Fig. 5. Vulnerability curves – Change of stem-specific hydraulic conductivity (K_s) in response to decreasing stem water potential (ψ, MPa) – of two-year-old seedlings of (a) *P. glauca,* (b) *P. mariana* and (c) *P. strobus*. Colored areas indicate the confidence intervals of the vulnerability curves. Vertical solid and dotted lines indicate the water potential leading to 50% loss of conductivity (P_{50}) and the confidence interval of the P_{50} respectively.

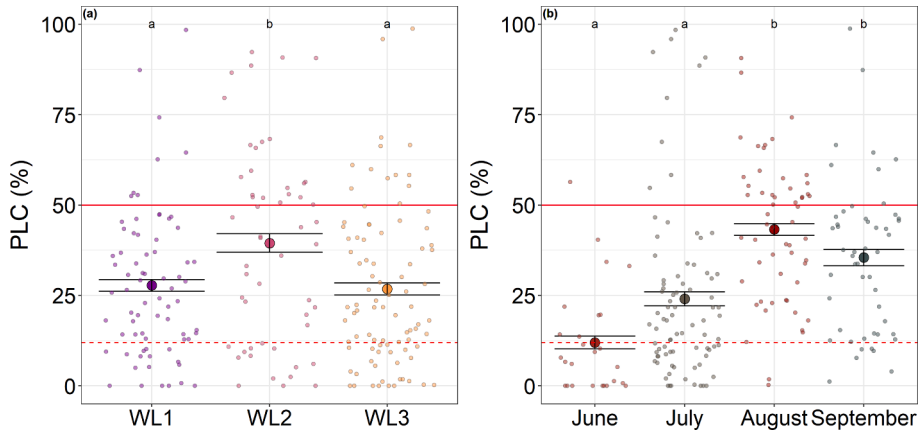

Fig. 6. Difference in native embolism (*PLC*) (a) among WL treatments and (b) over time. Means sharing the same lower-case letter indicate no significant difference ($\alpha < 0.05$). Data are presented as mean ± SE and jitter represents the distribution of the underlying data ($n \leq 171$ seedlings for (a) and $n \leq 144$ seedlings for (b)). Solid and dashed red lines indicate the thresholds of 50% and 12% loss of conductivity respectively.

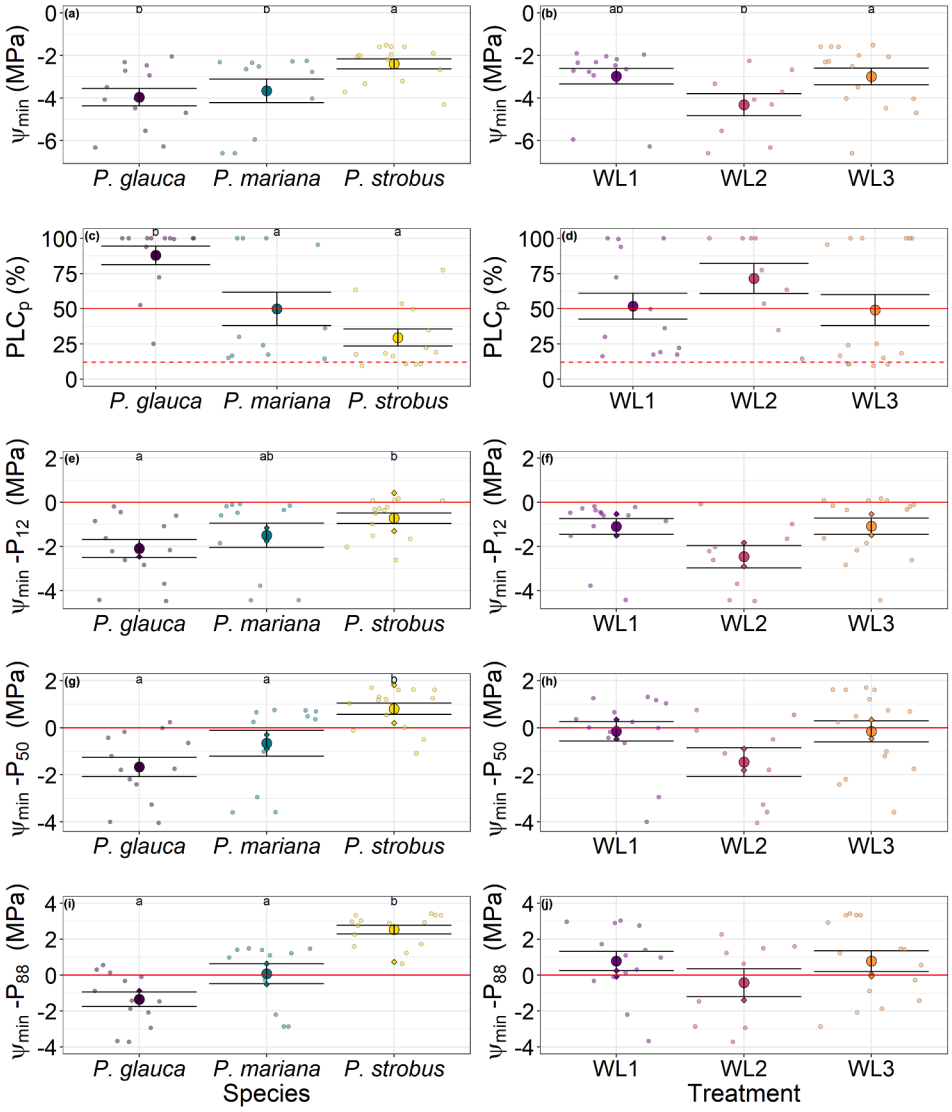

Fig. 7. Difference of (a, b) minimum seasonal water potential (Ψ_{min}), (c, d) predicted percent loss of conductivity (PLC_p), hydraulic safety margins (MPa) defined respectively with (e, f) P_{12}, (g, h) P_{50} and (i, j) P_{88} (a, c, e, g, i) among species and (b, d, f, h, j) among WL treatments. Solid and dashed red lines indicate the thresholds of 50% and 12% loss of conductivity respectively. Little diamond symbols indicate the mean hydraulic safety margin calculated with the lower or upper confidence interval of P_{12}, P_{50} or P_{88}. Solid red lines indicate a hydraulic safety margin equal to 0. Data are presented as mean ± SE and jitter represents the distribution of the underlying data ($n \leq 14$ seedlings for (a, c, e, g, i) and $n \leq 15$ seedlings (b, d, f, h, j)). Means sharing the same lower-case letter indicate no significant difference ($\alpha < 0.05$).

simulated potential future climates at the warmer edge of their regional distribution supports that drought stress is the main abiotic factor limiting tree survival for these populations (Hampe and Petit, 2005). These drought-induced mortality events could potentially lead to a range contraction at the southern edge of the species' distribution. Moreover, *P. strobus*, although at the core of its distribution in southern

Quebec, also experienced a high mortality rate, indicating a risk of extirpation of vulnerable populations in warmer and drier climates.

Our results are specific to seedlings, but we expect that mature trees of these species would be vulnerable in these future climate conditions as well. Although seedlings have shallower rooting depths, lower internal capacitance, and lower carbohydrate reserves than older trees, making them more vulnerable to drought, they also have lower water demand (Adams et al., 2017a). So, even if these species are only half as vulnerable to drought at the seedling or mature stages as we observed, we can still predict high mortality rate or regeneration failure in these forests in future warmer and drier environments. Moreover, as our experiment simulated hotter droughts in absence of biotic factors such as insects or pathogens (an unlikely condition in natural stands), future species risk is evident if the climate scenarios continue in the same path.

4.2. Species adaptive strategies to drought

Overall, the evolution of seedling water status during the growing season revealed how vulnerable to hotter drought the studied species will be in future drier and warmer climates and are in good agreement with mortality rates. All species (whatever the WL treatment) and all WL treatments (irrespective of species) presented a $PLC_p > 12\%$ and consequently, a negative $\psi_{min} - P_{12,}$ indicating that the threshold leading to a rapid increase of embolism was reached. Thus, a slight decrease of ψ_{min} highly increases the risk of runaway embolism (Meinzer et al., 2009), as shown by the native embolism measured at the end of the growing season (close to 50%). Moreover, *Picea* seedlings under all WL treatments reached negative (or equal to 0) $\psi_{min} - P_{50}$ and $\psi_{min} - P_{88}$, indicating that they likely functioned under the cavitation threshold leading to death (*i.e.,* ≥50% of embolism, see hereinafter). *P. strobus* presented greater (less negative for $\psi_{min} - P_{12}$ and positive for $\psi_{min} - P_{50}$ and $\psi_{min} - P_{88}$) safety margins due to a tendency to higher resistance to cavitation and less negative minimum water potentials compared to *Picea* species. The *Pinus* genus is known to have a high degree of isohydry, rapidly controlling stomatal conductance with increasing water stress (avoiding a high drop of water potential), whereas the strategy of *Picea* is considered intermediate; it exhibits a more anisohydric stomatal control (Dang et al., 1997). Species presenting a more isohydric strategy, such as *P. strobus*, would be more prone to suffer from carbon limitation in these conditions of successive droughts. Other mechanisms such as carbon starvation (the reduction of carbon gain due to stomatal closure), phloem transport failure, leaf, stem and meristem desiccation, could act in combination with hydraulic failure (Hajek et al., 2022; Mantova et al., 2021; McDowell et al., 2008, 2022; Mencuccini et al., 2015; Rowland et al., 2021), especially during successive periods of drought of lesser intensity. Isohydric species are more likely to optimize carbon assimilation during wet conditions, maintaining a large safety margin (Skelton et al., 2015).

4.3. The use of hydraulic safety margins to assess forest vulnerability to drought

Assessing drought-induced forest mortality comprises many challenges, as species have different adaptive strategies to drought. The use of other functional traits, such as the degree of isohydry, biomass partitioning, leaf and meristem relative water content (Mantova et al., 2022), in combination with hydraulic safety margins, would allow us to better predict vulnerability of forests to future droughts (Skelton et al., 2015). Nevertheless, hydraulic safety margins remain a powerful predictor to assess tree sensitivity to drought-induced mortality (Chen et al., 2022) of a population at a local or regional scale (e.g., Anderegg and HilleRisLambers, 2016; Arend et al., 2021; Urli et al., 2015) across various biomes with constrasting mean annual precipitations (Choat et al., 2012). Indeed, the definition of hydraulic safety margins is largely accepted by plant ecophysiologists. Hydraulic threshold is still debated, with varying values reported in different studies. Some suggest a threshold higher than 60% (Adams et al., 2017b; Hammond et al., 2019; Mantova et al., 2021) while others suggest P_{50} as a good proxy for conifer species (Brodribb and Cochard, 2009; Brodribb et al., 2010; Liang et al., 2021). However, differences in embolism resistance and rates of decline in water potential are likely the primary drivers affecting vulnerability to drought-induced mortality, rather than the lethal hydraulic threshold itself (Hammond et al., 2019). Hence, this tool could be useful as it indicates how close to its hydraulic dysfunction threshold the tree operates (Delzon and Cochard, 2014). For instance, Urli et al. (2015) found negative safety margins defined with P_{12} and P_{50} and narrow safety margin defined with P_{88} for *Quercus robur* L., a high heritage value species in a coastal forest in South-West France. Using these results and the quantification of the abundance of this species along a water gradient, they concluded that this population was highly vulnerable to drought-induced mortality and will be endangered in this ecosystem in the context of climate change. Thus, hydraulic safety margins may offer crucial information to forest practitioners so they can adapt forest management to climate change.

Some precautions are needed to properly determine the hydraulic safety margin, such as taking intraspecific variability of hydraulic traits as P_{12}, P_{50} and P_{88} into account. The confidence interval around P_{50} revealed that the hydraulic safety margin of *P. strobus* could be closer to 0, indicating higher vulnerability to drought in future warmer and drier climates. Indeed, Anderegg (2015) documented substantial intraspecific variability to resistance to cavitation within a species over space and time. Therefore, it is crucial to use P_{12}, P_{50} and P_{88} to define the hydraulic safety margins, determined on individuals of the same provenance, grown in the same conditions (field or controlled conditions) as those on which ψ_{min} is assessed. The development of new proxies for P_{50} of young conifer sapwood such as the water potential leading to 25% relative water loss (Rosner et al., 2021) is promising for the implementation of such precautions.

4.4. Conclusion

The originality of our study resides in the application, in a greenhouse experiment, of three realistic simulated future climate conditions that varied the intensity and frequency of droughts during a growing season. We assessed seedling responses of three economically and ecologically important species of this region to these different scenarios. Irrespective of the species and the frequency and intensity of droughts, the warmer and drier conditions in future predicted climates led to high mortality (higher than or close to 75% for all species in the WL treatments). Moreover, survivors at the end of the growing season were characterized by high levels of native embolism, which increases their probability of dying in the next growing seasons, since drought-induced embolism repair is usually impossible (Choat et al., 2015; Lamarque et al., 2018). The pattern of hydraulic safety is consistent with the pattern of mortality that we observed. This supports that adding hydraulic safety margin to a portfolio of functional traits could be relevant, as trait-based approaches are a promising avenue to assess species vulnerability to drought, and therefore guide and inform forest practitioners in species choice for adaptive silviculture (Boisvert-Marsh et al., 2020; Li et al., 2022). As drought is not and will not be the only threat to forest health in the context of global change, there is an urgent need to develop management strategies that will contribute to adapt northern temperate forests to climate change, as dominant conifer species are highly vulnerable to future warmer and drier climates.

5. Acknowlegments

We are indebted to Pierre-Nicolas Barbeau (Ministère des Forêts, de la Faune et des Parcs; MFFP), Ariane Belleau (Université Laval; UL), Hélène Chardin (UL), Raphaël Desrosiers (MFFP), Sébastien Dumont (UL), Caroline Durand (UL), Katherine Galibois (MFFP), Simon-Pierre Hamel (MFFP), Lena Levoy (MFFP), Simon Marcouiller (MFFP),

Marie-Andrée Paré (UL), Olivier Richard (MFFP), Zachary Sauvageau (MFFP), Karine Thériault (MFFP) and Rémi Van de Weghe (UL) for their help with the experiments. We thank Josianne Deblois (MFFP), Marie-Claude Lambert (MFFP) and Isabelle Auger (MFFP) for statistical advice, François Larochelle (UL) for his technical assistance with the greenhouse and Sylvie Carles (MFFP) for her scientific advice concerning the plant material. We thank two anonymous reviewers for their insightful comments during the review process of this manuscript. This work was funded by the Fonds Vert du Québec through a Contrat de recherche forestière obtained from the Ministère des Forêts, de la Faune et des Parcs (Quebec, Canada) by Alison Munson, as part of research project no. 142332161 of the Direction de la recherche forestière (project leader: Catherine Périé).

Author contributions

AM, CP and MU conceived this project. AM, CP, MC, MU, NT and TL designed the experiment. MC, AM, CP, NT, MU helped to conduct the experimentations. MC and MU helped with data collection. MU assumed data management and analysis. AM, CP, MC, MU, NT and SP discussed the results. MU wrote the original draft and all authors commented it.

Declaration of Competing Interest

The authors declare that they have no known competing financial interests or personal relationships that could have appeared to influence the work reported in this paper.

Data availability

The data that support the findings of this study are openly available in Figshare at https://doi.org/10.6084/m9.figshare.19694872.v3.

Appendix A. Supplementary data

Supplementary data to this article can be found online at https://doi.org/10.1016/j.foreco.2023.121127.

References

Adams, H.D., Barron-Gafford, G.A., Minor, R.L., Gardea, A.A., Bentley, L.P., Law, D.J., Breshears, D.D., McDowell, N.G., Huxman, T.E., 2017a. Temperature response surfaces for mortality risk of tree species with future drought. Environ. Res. Lett. 12 (11) https://doi.org/10.1088/1748-9326/aa93be.

Adams, H.D., Zeppel, M.J.B., Anderegg, W.R.L., Hartmann, H., Landhäusser, S.M., Tissue, D.T., Huxman, T.E., Hudson, P.J., Franz, T.E., Allen, C.D., Anderegg, L.D.L., Barron-Gafford, G.A., Beerling, D.J., Breshears, D.D., Brodribb, T.J., Bugmann, H., Cobb, R.C., Collins, A.D., Dickman, L.T., Duan, H., Ewers, B.E., Galiano, L., Galvez, D.A., Garcia-Forner, N., Gaylord, M.L., Germino, A.G., Gessler, A., Hacke, U. G., Hakamada, R., Hector, A., Jenkins, M.W., Kane, J.M., Kolb, T.E., Law, D.J., Lewis, J.D., Limousin, J.-M., Love, D.M., Macalady, A.K., Martinez-Vilalta, J., Mencuccini, M., Mitchell, P.J., Muss, J.D., O'Brien, M.J., O'Grady, A.P., Pangle, R.E., Pinkard, E.A., Piper, F.I., Plaut, J.A., Pockman, W.T., Quirk, J., Reinhardt, K., Ripullone, F., Ryan, M.G., Sala, A., Sevanto, S., Sperry, J.S., Vargas, R., Vennetier, M., Way, D.A., Xu, C., Yepez, E.A., McDowell, N.G., 2017b. A multi-species synthesis of physiological mechanisms in drought-induced tree mortality. Nat. Ecol. Evol. 1, 1285–1291. https://doi.org/10.1038/s41559-017-0248-x.

Agriculture et Agroalimentaire Canada Outil de surveillance des sécheresses au Canada [WWW Document] https://publications.gc.ca/site/archivee-archived.html?url=https://publications.gc.ca/collections/collection_2018/aac-aafc/A27-39-2012-7-fra.pdf 2012 accessed 4.20.22.

Allen, C.D., Breshears, D.D., McDowell, N.G., 2015. On underestimation of global vulnerability to tree mortality and forest die-off from hotter drought in the Anthropocene. Ecosphere 6, art129. https://doi.org/10.1890/ES15-00203.1.

Anderegg, W.R.L., 2015. Spatial and temporal variation in plant hydraulic traits and their relevance for climate change impacts on vegetation. New Phytol. 205, 1008–1014. https://doi.org/10.1111/nph.12907.

Anderegg, W.R.L., Hicke, J.A., Fisher, R.A., Allen, C.D., Aukema, J., Bentz, B., Hood, S., Lichstein, J.W., Macalady, A.K., McDowell, N., Pan, Y., Raffa, K., Sala, A., Shaw, J. D., Stephenson, N.L., Tague, C., Zeppel, M., 2015. Tree mortality from drought, insects, and their interactions in a changing climate. New Phytol. 208, 674–683. https://doi.org/10.1111/nph.13477.

Anderegg, L.D.L., HilleRisLambers, J., 2016. Drought stress limits the geographic ranges of two tree species via different physiological mechanisms. Glob. Chang. Biol. 22, 1029–1045. https://doi.org/10.1111/gcb.13148.

Anderegg, W.R.L., Klein, T., Bartlett, M., Sack, L., Pellegrini, A.F.A., Choat, B., Jansen, S., 2016. Meta-analysis reveals that hydraulic traits explain cross-species patterns of drought-induced tree mortality across the globe. PNAS 113, 5024–5029. https://doi.org/10.1073/pnas.1525678113.

M. Arend R.M. Link R. Patthey G. Hoch B. Schuldt A. Kahmen Rapid hydraulic collapse as cause of drought-induced mortality in conifers PNAS 118 2021 10.1073/pnas.2025251118 e2025251118.

Baier, W., Robertson, G.W., 1965. Estimation of latent evaporation from simple weather observations. Can. J. Plant Sci. 45, 276–284. https://doi.org/10.4141/cjps65-051.

Balducci, L., Deslauriers, A., Giovannelli, A., Beaulieu, M., Delzon, S., Rossi, S., Rathgeber, C.B.K., 2015. How do drought and warming influence survival and wood traits of Picea mariana saplings? J. Exp. Bot. 66, 377–389. https://doi.org/10.1093/jxb/eru431.

Bates, D., Mächler, M., Bolker, B., Walker, S., 2015. Fitting Linear Mixed-Effects Models Using lme4. J. Stat. Softw. 67, 1–48. https://doi.org/10.18637/jss.v067.i01.

Boisvert-Marsh, L., Royer-Tardif, S., Nolet, P., Doyon, F., Aubin, I., 2020. Using a trait-based approach to compare tree species sensitivity to climate change stressors in Eastern Canada and inform adaptation practices. Forests 11, 989. https://doi.org/10.3390/f11090989.

Breshears, D.D., Adams, H.D., Eamus, D., McDowell, N., Law, D.J., Will, R.E., Williams, A.P., Zou, C.B., 2013. The critical amplifying role of increasing atmospheric moisture demand on tree mortality and associated regional die-off. Front. Plant Sci. 4, 266. https://doi.org/10.3389/fpls.2013.00266.

Brodribb, T.J., Bowman, D.J., Nichols, S., Delzon, S., Burlett, R., 2010. Xylem function and growth rate interact to determine recovery rates after exposure to extreme water deficit. New Phytol. 188, 533–542. https://doi.org/10.1111/j.1469-8137.2010.03393.x.

Brodribb, T., Cochard, H., 2009. Hydraulic failure defines the recovery and point of death in water-stressed conifers. Plant Physiol. 149, 575–584. https://doi.org/10.1104/pp.108.129783.

Brodribb, T., Powers, J., Cochard, H., Choat, B., 2020. Hanging by a thread? Forests and drought. Science 368, 261–266. https://www.science.org/doi/10.1126/science.aat7631.

Burns, R.M., Honkala, B.H., 1990. Silvics of North America: 1. Conifers; 2. Hardwoods, Agriculture Handbook 654. U.S. Department of Agriculture, Forest Service, Wahington, DC.

Chen, Z., Li, S., Wan, X., Liu, S., 2022. Strategies of tree species to adapt to drought from leaf stomatal regulation and stem embolism resistance to root properties. Front Plant Sci 13. https://www.frontiersin.org/articles/10.3389/fpls.2022.926535.

Choat, B., Jansen, S., Brodribb, T.J., Cochard, H., Delzon, S., Bhaskar, R., Bucci, S.J., Feild, T.S., Gleason, S.M., Hacke, U.G., Jacobsen, A.L., Lens, F., Maherali, H., Martínez-Vilalta, J., Mayr, S., Mencuccini, M., Mitchell, P.J., Nardini, A., Pittermann, J., Pratt, R.B., Sperry, J.S., Westoby, M., Wright, I.J., Zanne, A.E., 2012. Global convergence in the vulnerability of forests to drought. Nature 491, 752–755. https://doi.org/10.1038/nature11688.

Choat, B., Brodersen, C.R., McElrone, A.J., 2015. Synchrotron X-ray microtomography of xylem embolism in Sequoia sempervirens saplings during cycles of drought and recovery. New Phytol. 205, 1095–1105. https://doi.org/10.1111/nph.13110.

Choat, B., Brodribb, T.J., Brodersen, C.R., Duursma, R.A., López, R., Medlyn, B.E., 2018. Triggers of tree mortality under drought. Nature 558, 531–539. https://doi.org/10.1038/s41586-018-0240-x.

Clark, J.S., Iverson, L., Woodall, C.W., Allen, C.D., Bell, D.M., Bragg, D.C., D'Amato, A. W., Davis, F.W., Hersh, M.H., Ibanez, I., Jackson, S.T., Matthews, S., Pederson, N., Peters, M., Schwartz, M.W., Waring, K.M., Zimmermann, N.E., 2016. The impacts of increasing drought on forest dynamics, structure, and biodiversity in the United States. Glob. Chang. Biol. 22, 2329–2352. https://doi.org/10.1111/gcb.13160.

Cornelissen, J.H.C., Lavorel, S., Garnier, E., Díaz, S., Buchmann, N., Gurvich, D.E., Reich, P.B., ter Steege, H., Morgan, H.D., van der Heijden, M.G.A., Pausas, J.G., Poorter, H., 2003. A handbook of protocols for standardised and easy measurement of plant functional traits worldwide. Aus. J. Bot. 51, 335–380. https://doi.org/10.1071/BT02124.

Dang, Q.-L., Margolis, H.A., Coyea, M.R., Sy, M., Collatz, G.J., 1997. Regulation of branch-level gas exchange of boreal trees: roles of shoot water potential and vapor pressure difference. Tree Phys. 17, 521–535. https://doi.org/10.1093/treephys/17.8-9.521.

Delzon, S., Cochard, H., 2014. Recent advances in tree hydraulics highlight the ecological significance of the hydraulic safety margin. New Phytol. 203, 355–358. https://doi.org/10.1111/nph.12798.

Duursma, R., Choat, B., 2017. fitplc - an R package to fit hydraulic vulnerability curves. J. Plant. Hydraul. 4, 002. https://doi.org/10.20870/jph.2017.e002.

Environment and Climate Change Canada, 2018. Données climatiques historiques [WWW Document]. URL https://climat.meteo.gc.ca/historical_data/search_historic_data_f.html (accessed 7.23.18).

Gauthier, S., Bernier, P., Burton, P.J., Edwards, J., Isaac, K., Isabel, N., Jayen, K., Le Goff, H., Nelson, E.A., 2014. Climate change vulnerability and adaptation in the managed Canadian boreal forest. Environ. Rev. 22, 256–285. https://doi.org/10.1139/er-2013-0064.

Hajek, P., Link, R.M., Nock, C., Bauhus, J., Gebauer, T., Gessler, A., Kovach, K., Messier, C., Paquette, A., Saurer, M., Scherer-Lorenzen, M., Rose, L., Schuldt, B., 2022. Mutually inclusive mechanisms of drought-induced tree mortality. Glob. Chang. Biol. 00, 1–14. https://doi.org/10.1111/gcb.16146.

Hammond, W.M., Yu, K.L., Wilson, L.A., Will, R.E., Anderegg, W.R.L., Adams, H.D., 2019. Dead or dying? Quantifying the point of no return from hydraulic failure in

drought-induced tree mortality. New Phytol. 223, 1834–1843. https://doi.org/10.1111/nph.15922.
Hammond, W.M., Williams, A.P., Abatzoglou, J.T., Adams, H.D., Klein, T., Lopez Rodriguez, R., Saenz-Romero, C., Hartmann, H., Breshears, D., Allen, C.D., 2022. Global field observations of tree die-off reveal hotter-drought fingerprint for Earth's forests. Nat. Commun. 13, 1761. https://doi.org/10.1038/s41467-022-29289-2.
Hampe, A., Petit, R.J., 2005. Conserving biodiversity under climate change: the rear edge matters. Ecol. Lett. 8, 461–467. https://doi.org/10.1111/j.1461-0248.2005.00739.x.
Hartmann, H., Bastos, A., Das, A.J., Esquivel-Muelbert, A., Hammond, W.M., Martínez-Vilalta, J., McDowell, N.G., Powers, J.S., Pugh, T.A.M., Ruthrof, K.X., Allen, C.D., 2022. Climate change risks to global forest health: emergence of unexpected events of elevated tree mortality worldwide. Annu. Rev. Plant Biol. 73 (1), 673–702.
Kuznetsova, A., Brockhoff, P.B., Christensen, R.H.B., 2017. lmerTest Package: Tests in Linear Mixed Effects Models. J. Stat. Softw. 82, 1–26. https://doi.org/10.18637/jss.v082.i13.
Laflamme, J., Munson, A.D., Grondin, P., Arseneault, D., 2016. Anthropogenic disturbances create a new vegetation toposequence in the Gatineau River Valley. Quebec Forests 7, 254. https://doi.org/10.3390/f7110254.
Lamarque, L.J., Corso, D., Torres-Ruiz, J.M., Badel, E., Brodribb, T.J., Burlett, R., Charrier, G., Choat, B., Cochard, H., Gambetta, G.A., Jansen, S., King, A., Lenoir, N., Martin-StPaul, N., Steppe, K., Van den Bulcke, J., Zhang, Y., Delzon, S., 2018. An inconvenient truth about xylem resistance to embolism in the model species for refilling Laurus nobilis L. Ann. For. Sci. 75, 88. https://doi.org/10.1007/s13595-018-0768-9.
Lenth, R., 2021. Estimated Marginal Means, aka Least-Squares Means [WWW Document]. URL https://github.com/rvlenth/emmeans (accessed 4.22.21).
Li, X., Xi, B., Wu, X., Choat, B., Feng, J., Jiang, M., Tissue, D., 2022. Unlocking drought-induced tree mortality: physiological mechanisms to modeling. Front. Plant Sci. 13, 835921 https://doi.org/10.3389/fpls.2022.835921.
Liang, X., Ye, Q., Liu, H., Brodribb, T.J., 2021. Wood density predicts mortality threshold for diverse trees. New Phytol. 229, 3053–3057. https://doi.org/10.1111/nph.17117.
Littell, R.C., Milliken, G.A., Stroup, W.W., Wolfinger, R.D., Schabenberger, O., 2006. SAS System for Mixed Models, Second Edition. SAS Institute Inc., Cary, NC.
Mantova, M., Menezes-Silva, P.E., Badel, E., Cochard, H., Torres-Ruiz, J.M., 2021. The interplay of hydraulic failure and cell vitality explains tree capacity to recover from drought. Physiol. Plant. 172, 247–257. https://doi.org/10.1111/ppl.13331.
Mantova, M., Herbette, S., Cochard, H., Torres-Ruiz, J.M., 2022. Hydraulic failure and tree mortality: from correlation to causation. Trends Plant Sci. 27, 335–345. https://doi.org/10.1016/j.tplants.2021.10.003.
Martin-StPaul, N., Delzon, S., Cochard, H., Maherali, H., 2017. Plant resistance to drought depends on timely stomatal closure. Ecol. Lett. 20 (11), 1437–1447.
Martynov, A., Laprise, R., Sushama, L., Winger, K., Šeparović, L., Dugas, B., 2013. Reanalysis-driven climate simulation over CORDEX North America domain using the Canadian Regional Climate Model, version 5: model performance evaluation. Clim. Dyn. 41, 2973–3005. https://doi.org/10.1007/s00382-013-1778-9.
McDowell, N.G., Allen, C.D., 2015. Darcy's law predicts widespread forest mortality under climate warming. Nat. Clim. Chang. 5, 669–672. https://www.nature.com/articles/nclimate2641.
McDowell, N., Pockman, W.T., Allen, C.D., Breshears, D.D., Cobb, N., Kolb, T., Plaut, J., Sperry, J., West, A., Williams, D.G., Yepez, E.A., 2008. Mechanisms of plant survival and mortality during drought: why do some plants survive while others succumb to drought? New Phytol. 178, 719–739. https://doi.org/10.1111/j.1469-8137.2008.02436.x.
McDowell, N.G., Sapes, G., Pivovaroff, A., Adams, H.D., Allen, C.D., Anderegg, W.R.L., Arend, M., Breshears, D.D., Brodribb, T., Choat, B., Cochard, H., De Cáceres, M., De Kauwe, M.G., Grossiord, C., Hammond, W.M., Hartmann, H., Hoch, G., Kahmen, A., Klein, T., Mackay, D.S., Mantova, M., Martínez-Vilalta, J., Medlyn, B.E., Mencuccini, M., Nardini, A., Oliveira, R.S., Sala, A., Tissue, D.T., Torres-Ruiz, J.M., Trowbridge, A.M., Trugman, A.T., Wiley, E., Xu, C., 2022. Mechanisms of woody-plant mortality under rising drought, CO_2 and vapour pressure deficit. Nat. Rev. Earth Environ. 3 (5), 294–308.
Meinshausen, M., Smith, S.J., Calvin, K., Daniel, J.S., Kainuma, M.L.T., Lamarque, J.-F., Matsumoto, K., Montzka, S.A., Raper, S.C.B., Riahi, K., Thomson, A., Velders, G.J.M., van Vuuren, D.P.P., 2011. The RCP greenhouse gas concentrations and their extensions from 1765 to 2300. Clim. Change 109 (1-2), 213–241.
Meinzer, F.C., Johnson, D.M., Lachenbruch, B., McCulloh, K.A., Woodruff, D.R., 2009. Xylem hydraulic safety margins in woody plants: coordination of stomatal control of xylem tension with hydraulic capacitance. Funct. Ecol. 23, 922–930. https://doi.org/10.1111/j.1365-2435.2009.01577.x.
Melcher, P.J., Michele Holbrook, N., Burns, M.J., Zwieniecki, M.A., Cobb, A.R., Brodribb, T.J., Choat, B., Sack, L., 2012. Measurements of stem xylem hydraulic conductivity in the laboratory and field. Methods Ecol. Evol. 3, 685–694. https://doi.org/10.1111/j.2041-210X.2012.00204.x.
Mencuccini, M., Minunno, F., Salmon, Y., Martínez-Vilalta, J., Hölttä, T., 2015. Coordination of physiological traits involved in drought-induced mortality of woody plants. New Phytol. 208, 396–409. https://doi.org/10.1111/nph.13461.
Ministère des Forêts de la Faune et des Parcs, 2020. Ressources et industries forestières du Québec, Portrait statistique, Ministère des Forêts 2019 de la Faune et des Parcs Québec, QC, Canada.
Ministère des Ressources naturelles, 2012. Insectes, maladies et feux dans les forêts québécoises [WWW Document]. URL www.mrn.gouv.qc.ca/forets/fimaq/publications/index.jsp (accessed 4.20.22).
Moss, R.H., Edmonds, J.A., Hibbard, K.A., Manning, M.R., Rose, S.K., van Vuuren, D.P., Carter, T.R., Emori, S., Kainuma, M., Kram, T., Meehl, G.A., Mitchell, J.F., Nakicenovic, N., Riahi, K., Smith, S.J., Stouffer, R.J., Thomson, A.M., Weyant, J.P., Wilbanks, T.J., 2010. The next generation of scenarios for climate change research and assessment. Nature 463, 747–756. https://doi.org/10.1038/nature08823.
Ouranos, Vers l'adaptation. Synthèse des connaissances sur les changements climatiques au Québec Editions 2015. ed. 2015 Ouranos, Montréal, Québec.
Périé, C., de Blois, S., 2016. Dominant forest tree species are potentially vulnerable to climate change over large portions of their range even at high latitudes. PeerJ 4, e2218. https://peerj.com/articles/2218/.
Périé, C., de Blois, S., Lambert, M.-C., 2009. Atlas interactif : Changements climatiques et habitats des arbres [base de données]. [WWW Document]. URL https://mffp.gouv.qc.ca/changements-climatiques/outil/carte.html (accessed 10.31.21).
R Core Team, 2020. R: A language and environment for statistical computing. R Foundation for Statistical Computing, Vienna, Austria.
Reich, P.B., Bermudez, R., Montgomery, R.A., Rich, R.L., Rice, K.E., Hobbie, S.E., Stefanski, A., 2022. Even modest climate change may lead to major transitions in boreal forests. Nature 608, 540–545. https://doi.org/10.1038/s41586-022-05076-3.
Rochette, P., Dubé, P.-A., 1989. Calibration d'une équation simple pour l'estimation de l'évapotranspiration potentielle. Nat. Can. 116, 193–203.
Rosner, S., Nöbauer, S., Voggeneder, K., 2021. Ready for screening: fast assessable hydraulic and anatomical proxies for vulnerability to cavitation of young conifer sapwood. Forests 12, 1104. https://doi.org/10.3390/f12081104.
Rowland, L., Martínez-Vilalta, J., Mencuccini, M., 2021. Hard times for high expectations from hydraulics: predicting drought-induced forest mortality at landscape scales remains a challenge. New Phytol. 230, 1685–1687. https://doi.org/10.1111/nph.17317.
Sack, L., Bartlett, M.K., Creese, C., Guyot, G., Scoffoni, C., PrometheusWiki contributors, 2011. Constructing and operating a hydraulic flow meter [WWW Document]. URL https://prometheuswiki.rsb.anu.edu.au/tiki-index.php?page=Constructing+and+operating+a+hydraulics+flow+meter (accessed 9.30.18).
Saucier, J.-P., Robitaille, A., Grondin, P., 2009. Cadre bioclimatique du Québec, in: Manuel de Foresterie, 2nd Ed. R. Doucet and M. Côté. Ordre des ingénieurs forestiers du Québec, Éditions Multimondes, Québec, Québec, pp. 186–205.
Šeparović, L., Alexandru, A., Laprise, R., Martynov, A., Sushama, L., Winger, K., Tete, K., Valin, M., 2013. Present climate and climate change over North America as simulated by the fifth-generation Canadian regional climate model. Clim. Dyn. 41, 3167–3201. https://doi.org/10.1007/s00382-013-1737-5.
Skelton, R.P., West, A.G., Dawson, T.E., 2015. Predicting plant vulnerability to drought in biodiverse regions using functional traits. PNAS 112, 5744–5749. https://doi.org/10.1073/pnas.1503376112.
Skelton, R.P., Brodribb, T.J., McAdam, S.A.M., Mitchell, P.J., 2017. Gas exchange recovery following natural drought is rapid unless limited by loss of leaf hydraulic conductance: evidence from an evergreen woodland. New Phytol. 215, 1399–1412. https://doi.org/10.1111/nph.14652.
Stroock, A.D., Pagay, V.V., Zwieniecki, M.A., Michele Holbrook, N., 2014. The Physicochemical Hydrodynamics of Vascular Plants. Annu. Rev. Fluid Mech. 46, 615–642. https://doi.org/10.1146/annurev-fluid-010313-141411.
Thompson, R.S., Anderson, K.H., Bartlein, P.J., 1999. Atlas of relations between climatic parameters and distributions of important trees and shrubs in North America, U.S. Geological Survey Professional Paper 1650-A. USGS, Denver, CO, USA.
Urli, M., Périé, C., Thiffault, N., Coyea, M.R., Pepin, S., Lambert, M.-C., Munson, A.D., under review. On the need to report the variability and data used in the determination of xylem vulnerability curve parameters. J Plant Hydraul.
Urli, M., Porte, A.J., Cochard, H., Guengant, Y., Burlett, R., Delzon, S., 2013. Xylem embolism threshold for catastrophic hydraulic failure in angiosperm trees. Tree Phys. 33 (7), 672–683.
Urli, M., Lamy, J.-B., Sin, F., Burlett, R., Delzon, S., Porté, A.J., 2015. The high vulnerability of Quercus robur to drought at its southern margin paves the way for Quercus ilex. Plant Ecol. 216, 177–187. https://doi.org/10.1007/s11258-014-0426-8.
Waring, R.H., 1987. Characteristics of trees predisposed to die. Bioscience 37, 569–574. https://doi.org/10.2307/1310667.